Biophysical Journal
Article

Biophysical Society

Omecamtiv Mecarbil Slows Myosin Kinetics in Skinned Rat Myocardium at Physiological Temperature

Thinh T. Kieu,[1] Peter O. Awinda,[1] and Bertrand C. W. Tanner[1,2,*]
[1]Department of Integrative Physiology and Neuroscience and [2]Washington Center for Muscle Biology, Washington State University, Pullman, Washington

ABSTRACT Heart failure is a life-threatening condition that occurs when the heart muscle becomes weakened and cannot adequately circulate blood and nutrients around the body. Omecamtiv mecarbil (OM) is a compound that has been developed to treat systolic heart failure via targeting the cardiac myosin heavy chain to increase myocardial contractility. Biophysical and biochemical studies have found that OM increases calcium (Ca^{2+}) sensitivity of contraction by prolonging the myosin working stroke and increasing the actin-myosin cross-bridge duty ratio. Most in vitro studies probing the effects of OM on cross-bridge kinetics and muscle force production have been conducted at subphysiological temperature, even though temperature plays a critical role in enzyme activity and cross-bridge function. Herein, we used skinned, ventricular papillary muscle strips from rats to investigate the effects of [OM] on Ca^{2+}-activated force production, cross-bridge kinetics, and myocardial viscoelasticity at physiological temperature (37°C). We find that OM only increases myocardial contractility at submaximal Ca^{2+} activation levels and not maximal Ca^{2+} activation levels. As [OM] increased, the kinetic rate constants for cross-bridge recruitment and detachment slowed for both submaximal and maximal Ca^{2+}-activated conditions. These findings support a mechanism by which OM increases cardiac contractility at physiological temperature via increasing cross-bridge contributions to thin-filament activation as cross-bridge kinetics slow and the duration of cross-bridge attachment increases. Thus, force only increases at submaximal Ca^{2+} activation due to cooperative recruitment of neighboring cross-bridges, because thin-filament activation is not already saturated. In contrast, OM does not increase myocardial force production for maximal Ca^{2+}-activated conditions at physiological temperature because cooperative activation of thin filaments may already be saturated.

SIGNIFICANCE Omecamtiv mecarbil is a drug that increases cardiac force production via binding to the myosin cross-bridge, which was developed to as a therapy to treat systolic heart failure. Nearly all the prior biophysical studies of omecamtiv mecarbil on cardiac myosin and myocardial contractility occurred at sub-physiological temperature, which may be a contributing experimental factor that is limiting a clear understanding of the physiological impact of omecamtiv mecarbil on myosin cross-bridge function. Thus, we used skinned, ventricular papillary muscle strips from rats to investigate the effects of omecamtiv mecarbil on Ca^{2+}-activated force production, cross-bridge kinetics, and myocardial viscoelasticity at physiological temperature (37°C). Our findings indicate that omecamtiv mecarbil increases cardiac contractility solely at sub-maximal calcium levels.

INTRODUCTION

The transient interactions between the motor protein myosin along the thick filaments and actin proteins along the thin filaments of a cardiac muscle cell provide the force and shortening required to pump blood around the body. These actin-myosin cross-bridge interactions are Ca^{2+} regulated by thin-filament regulatory proteins (troponin and tropomyosin), and cross-bridge cycling is energetically driven by ATP hydrolysis (1). The hydrolysis products (ADP and inorganic phosphate, P_i) play critical chemomechanical roles underlying cross-bridge force production. In particular, the myosin powerstroke is generally associated with the release of inorganic phosphate from the myosin head, whereas myosin dissociation from actin is rate-limited by the detachment of ADP from myosin under physiological [Ca^{2+}] and

Submitted July 16, 2018, and accepted for publication April 15, 2019.
*Correspondence: bertrand.tanner@wsu.edu
Editor: Michael Ostap.
https://doi.org/10.1016/j.bpj.2019.04.020

[ATP] (1,2). Thus, there is a tight link between cross-bridge cycling kinetics and cardiac contractility.

Heart failure is a life-threatening condition that afflicts 6.5 million people above the age of 20 in the United States (3). Heart failure is the inability to provide sufficient cardiac output at normal filling pressures, thereby compromising the ability of the heart to pump enough blood to adequately meet required demands of the body. The two primary types of heart failure stem from systolic or diastolic dysfunction, and each represent roughly half of the heart failure population (3–6). Heart failure with reduced ejection fraction arises in patients when myocardial force production decreases (i.e., systolic dysfunction). Heart failure with preserved ejection fraction arises in patients when myocardial force production is preserved, but the heart cannot sufficiently relax to adequately fill with blood (i.e., diastolic dysfunction). Effective therapeutic treatments for heart failure remain limited, and current clinical strategies focus largely on lifestyle changes, a limited number of cardiac surgeries or transplants, and symptomatic therapeutic treatments of heart failure risk factors.

Recently, the pharmaceutical compound omecamtiv mecarbil (OM) was developed to combat systolic heart failure (7). OM brings exciting therapeutic potential in humans and animals, and it is currently in phase three clinical trials (8). In humans, OM has been shown to enhance systolic stroke volume, ejection fraction, fractional shortening, and ejection time (7,9,10). In animal models of cardiac function, prior studies have shown that OM increases Ca^{2+} sensitivity of contraction in cardiac muscle strips, promotes cross-bridge binding, stabilizes the prepowerstroke state of the motor domain, and accelerates P_i release from the myosin head (11–15). It has also been suggested that OM prolongs the duration of myosin cross-bridge attachment to increase the population of force-generating myosin heads and/or increase the myosin duty ratio (16–20). However, most biophysical studies of OM effects on contractility have used in vitro measurements at subphysiological temperature. In this study, we illustrate consistent effects of OM at physiological temperature (37°C) in skinned rat myocardial strips. Our findings indicate that OM-mediated increases in isometric force occur solely at submaximal calcium levels, due in part to slowed cross-bridge cycling kinetics. In agreement with prior studies (16–18,21,22), our findings support a mechanism by which OM increases cardiac contractility at physiological temperature via cross-bridge contributions to thin-filament activation from a slower-cycling population of cross-bridges (that are binding OM).

MATERIALS AND METHODS

Animal models

Experiments were conducted following the Guide for the Use and Care of Laboratory Animals published by the National Institutes of Health. Procedures were approved by the Institutional Animal Care and Use Committee at Washington State University. Five male Sprague-Dawley rats (18–26 weeks old) were acquired from Simonsen Laboratories (Gilroy, CA). Rats were anesthetized by isoflurane inhalation (3% volume in 95% O_2/5% CO_2 flowing at 2 L/min). Hearts were excised and immediately placed in dissecting solution on ice.

Muscle mechanics solutions

Methods and solutions for muscle mechanics measurements were adapted from our prior studies (23,24), with solution formulations calculated via solving ionic equilibria according to Godt and Lindley (25). All concentrations are listed in mM unless otherwise noted. Dissecting solution consisted of the following: 50 N,N-Bis(2-hydroxyethyl)-2-aminoethanesulfonic acid, N,N-bis(2-hydroxyethyl)taurine; 30.83 K propionate; 10 Na azide; 20 EGTA; 6.29 $MgCl_2$; 6.09 ATP; 1 1,4-dithiothreitol; 20 2,3-butanedione-monoxime; 50 μM leupeptin; 275 μM pefabloc; and 1 μM trans-epoxysuccinyl-L-leucylamido(4-guanidino)butane. Skinning solution consisted of the following: dissecting solution with 1% Triton-XT wt/vol and 50% glycerol wt/vol. Storage solution consisted of the following: dissecting solution with 50% glycerol wt/vol. Relaxing solution consisted of the following: pCa 8.0 ($pCa = -\log_{10}[Ca^{2+}]$); 20 N,N-Bis(2-hydroxyethyl)-2-aminoethanesulfonic acid, N,N-bis(2-hydroxyethyl)taurine; 5 EGTA; 5 MgATP; 1 Mg^{2+}; 0.3 P_i; 35 phosphocreatine; 300 U/mL creatine kinase; 200 ionic strength adjusted with Na methanesulfonate (pH 7.0). Maximal Ca^{2+}-activating solution was the same as the relaxing solution with pCa 4.8. Submaximal Ca^{2+}-activating solution was the same as the relaxing solution with pCa 5.4. These relaxing and activating solutions were originally made without any added OM. OM was purchased from AdooQ Biosciences (Irvine, CA), and a 10 mM OM stock solution was made by dissolving OM in dimethylsulfoxide (DMSO).

To make all required activating and relaxing solution (at appropriate [OM] or the appropriate control solution matching %DMSO-only concentration), the 10 mM OM stock was diluted into relaxing (pCa 8) and Ca^{2+}-activating solutions (pCa 5.4 and 4.8). These relaxing and activating solutions at intermediate [OM] were then used for solution exchange during the force-pCa curves or [OM] titration curves as needed (at three [OM] = 0.1, 1.0, and 10 μM, each containing 0.001, 0.01, and 0.1% DMSO in the exchange solutions, respectively). The tension-pCa experiments only used pCa 8.0 and 4.8 solutions. These OM-titration experiments used pCa 8.0, 5.4, and/or 4.8 solutions as needed, with intermediate exchange solutions being mixed proportionally to activate the myocardial strips across a range of [OM] at pCa 5.4 and 4.8. Control experiments matched %DMSO concentrations in all solutions, without any OM, to ensure equal amounts of DMSO were present between all appropriate paired groups of experiments. Among all experiments, DMSO was $\leq$0.1% solution volume. We do not anticipate that these low DMSO concentrations introduced any significant impact on the measured effects of [OM] described herein, even though DMSO has been shown to depress twitch forces (above ~5–10%) and skinned muscle force-pCa relationships (above ~1%) (26–28).

Skinned papillary mechanics

Left ventricular papillary muscles were dissected from five hearts and pared down to thin strips (~180 μm in diameter and 700 μm long). Strips were skinned overnight at 4°C, transferred to storage solution, and stored at −20°C for up to 1 week. Aluminum T-clips were attached to both ends of the strip, lowered into a 30 μL bubble of pCa 8.0 relaxing solution (surrounded by mineral oil in the experimental chamber), and then mounted between a piezoelectric motor (P841.40; Physik Instrumente, Auburn, MA) and a strain gauge (AE801; Kronex, Walnut Creek, CA). Next, the strip was stretched to 2.2 μm sarcomere length, measured by digital Fourier transform (IonOptix, Milton, MA). Dimensions of the skinned myocardial strips were then measured at 80× magnification. Cross-sectional area is

estimated as an ellipse, using the major and minor diameters (i.e., top width and side width) of each strip to normalize force differences between each preparation (tensile stress = force/cross-sectional area). Temperature was maintained at physiological temperature (37°C) throughout each experiment.

Strips were Ca^{2+} activated from pCa 8.0 to 4.8 to assess the tension-pCa relationships at 0, 0.1 and 1 μM [OM] (n listed in Table 1). A subset of these control strips (0 μM OM), after the pCa curve, underwent either a control titration (0–0.1% DMSO) or an OM titration (0–10 μM [OM]) at pCa 4.8 or 5.4. Additional strips were Ca^{2+} activated from pCa 8.0 directly to pCa 4.8 (in the absence of OM), and then a control or OM titration was performed at pCa 4.8 or 5.4. Number of strips for each condition are listed in figure legends.

Dynamic mechanical analysis

Stochastic length perturbations were applied for a period of 60 s, using an amplitude distribution with an SD of 0.05% muscle length over the frequency range of 0.25–250 Hz (24). Elastic and viscous moduli, E(ω) and V(ω), were measured as a function of angular frequency (ω) from the in-phase and out-of-phase portions of the tension response to the stochastic length perturbation. The complex modulus, Y(ω), was defined as E(ω) + iV(ω), where $i = \sqrt{-1}$. Moduli data from individual strips were fitted to Eq. 1. to estimate six model parameters (A, k, B, $2\pi b$, C, $2\pi c$) (29,30).

$$Y(\omega) = A(i\omega)^k - B\left(\frac{i\omega}{2\pi b + i\omega}\right) + C\left(\frac{i\omega}{2\pi c + i\omega}\right) \quad (1)$$

The A-term in Eq. 1 reflects the viscoelastic mechanical response of passive, structural elements in the muscle and holds no enzymatic dependence. The parameter A represents the combined mechanical stress of the strip, whereas the parameter k describes the viscoelasticity of these passive elements, where $k = 0$ represents a purely elastic response and $k = 1$ is a purely viscous response (31). The B and C terms in Eq. 1 reflect enzymatic cross-bridge cycling behavior that produce frequency-dependent shifts in the viscoelastic mechanical response during Ca^{2+}-activated contraction. These B and C processes characterize work-producing (cross-bridge recruitment and force-generating processes (29,32–34)) and work-absorbing (cross-bridge detachment and force decaying/decreasing processes (30)) muscle responses, respectively. The parameters B and C represent the mechanical stress from changes in cross-bridge binding/cycling, and the rate parameters $2\pi b$ and $2\pi c$ reflect cross-bridge kinetics that are sensitive to biochemical perturbations affecting enzymatic activity, such as [MgATP], [MgADP], or [Pi]. In combination, the molecular processes contributing to cross-bridge force generation underlie the rate constant for cross-bridge recruitment, $2\pi b$ (29,32–34), and processes contributing to cross-bridge detachment or force decay underlie the rate constant for cross-bridge detachment, $2\pi c$ (30).

TABLE 1 Characteristics of the Isometric Tension-pCa Relationships as [OM] Varied, Mean ± Standard Error

	0 μM OM	0.1 μM OM	1 μM OM
T_{min} (kN m^{-2})	2.55 ± 0.47	2.11 ± 0.58	2.33 ± 0.27
T_{max} (kN m^{-2})	24.70 ± 1.39	24.00 ± 1.54	27.1 ± 0.83
pCa_{50}	5.39 ± 0.02	5.44 ± 0.03	5.63 ± 0.04[a]
n_H	3.64 ± 0.31	3.32 ± 0.43	2.20 ± 0.10[a]
Max_{fit} (kN m^{-2})	22.96 ± 1.24	22.84 ± 1.27	25.73 ± 0.79
n strips	16	8	9

T_{min}, absolute tension value at pCa 8.0. T_{max}, absolute tension value at pCa 4.8. Max_{fit}, pCa_{50}, and n_H represent fit parameters to a three-parameter Hill equation for the Ca^{2+}-activated tension versus pCa relationship: $T(pCa) = (Max_{fit}/1 + 10^{n_H(pCa - pCa50)})$. Max_{fit} describes the asymptotic, maximal force value for the Ca^{2+}-activated developed tension-pCa response (where developed tension $T(pCa) = T_{absolute}(pCa) - T_{min}$). pCa_{50} represents the [Ca^{2+}] concentration at half-maximal tension ($pCa = -\log_{10}[Ca^{2+}]$). The Hill coefficient, n_H, is the slope the tension-pCa relationship at pCa_{50}; it represents the cooperativity coefficient of contractile activation in the myocardial strip.

[a]$p < 0.05$ effect of [OM] compared to 0 μM OM.

Statistical analysis

All data are listed or plotted as mean ± standard error. Constrained nonlinear least-squares fitting of moduli data to Eq. 1 was performed using sequential quadratic programming methods in Matlab (v.7.9.0; The MathWorks, Natick, MA). The effects of OM on each parameter were analyzed using linear mixed models with main effects of OM, the experimental group, and their interaction using SPSS (IBM Statistical, Chicago, IL).

RESULTS

Effects of [OM] on the isometric tension-pCa relationship

As [Ca^{2+}] increased from pCa 8.0 to 4.8, isometric tension increased in a sigmoidal manner, which was fit to a three-parameter Hill equation (Table 1). At 1.0 μM [OM], there was a leftward shift in the tension-pCa relationship compared to 0 μM [OM], indicating an increase in Ca^{2+} sensitivity of contraction due to OM (Fig. 1). The 1.0 μM [OM] also produced ~40% decrease in the slope of the tension-pCa-relationship (vs. 0 μM [OM]), primarily due to increased contractility at submaximal activation levels, which shifted the bottom portion of the tension-pCa relationship to the left. Although 0.1 μM [OM] produced a subtle leftward shift in the tension-pCa relationship, there were no statistically significant effects on steady-state isometric contraction between 0 and 0.1 μM [OM]. There were no

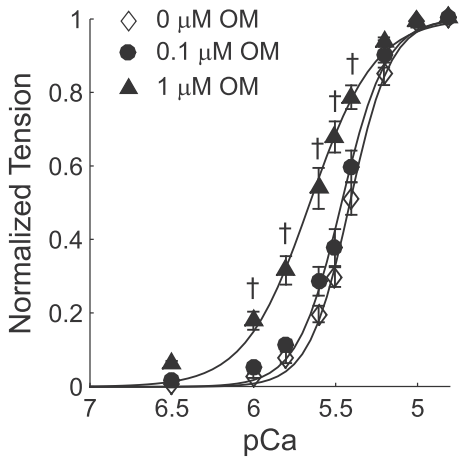

FIGURE 1 Effects of 0, 0.1, and 1 μM OM on the steady-state isometric tension-pCa relationships. Data were normalized to the maximal Ca^{2+} activated tension value (at pCa 4.8) within each group, and lines represent three-parameter Hill fits. Number of strips for each condition are listed in Table 1. †$p < 0.05$ for 1 μM OM versus the other two conditions, which were not statistically different at any pCa level.

significant differences in relaxed (pCa 8.0) nor maximally activated (pCa 4.8) tension values (Table 1) among these average tension-pCa responses at the three [OM].

Effects of [OM] on steady-state isometric tension at maximal and submaximal Ca^{2+} activation

Fig. 2 illustrates the isometric tension response to increasing [OM] (from 0 to 10 μM) at pCa 4.8 (Fig. 2 *A*) and 5.4 (Fig. 2 *B*). Data were normalized to the 0 μM [OM] within each pCa level, just before the OM-titration curve; these steady-state isometric tension values did not differ between the OM and control strips within each pCa level. Specifically, the tension values used for normalization were 1) 22.6 $\pm$ 1.0 and 20.7 $\pm$ 1.1 kPa at pCa 4.8 for OM and control strips, respectively, and 2) 9.7 $\pm$ 0.8 and 11.8 $\pm$ 0.8 kPa at pCa 5.4 for OM and control strips, respectively. There were not significant changes in steady-state tension measurements for the control (DMSO-only; 0–0.01% DMSO) across the range of solution exchanges within each pCa level. At maximal Ca^{2+} activation (pCa 4.8; Fig. 2 *A*), isometric tension was not affected by [OM] $\leq$ 3 μM, but tension decreased by ~30% at 10 μM [OM]. In contrast, at submaximal Ca^{2+} activation (Fig. 2 *B*; pCa 5.4), isometric tension increased in a biphasic manner as [OM] increased, showing the greatest tension increase at 3 μM [OM]. This biphasic [OM]-tension response was consistent with previous findings in myocardial strips from rat (14,16) and guinea pig (35).

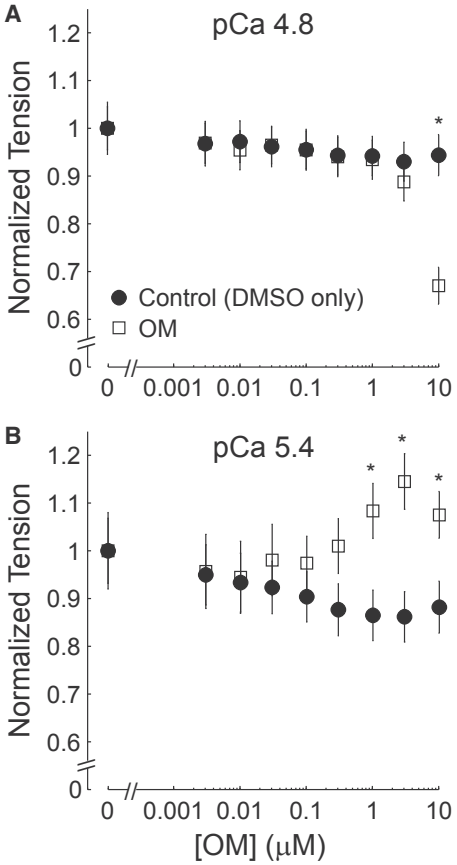

FIGURE 2 Steady-state isometric tension values were plotted against [OM] at pCa 4.8 (*A*) and pCa 5.4 (*B*). Data were normalized to Ca^{2+}-activated tension value at 0 μM [OM] within each group. Number of strips: 13 control at pCa 4.8, 21 OM at pCa 4.8, 12 control at pCa 5.4, 20 OM at pCa 5.4. *$p < 0.05$ between the control and OM titration within each panel.

Effects of [OM] on myocardial viscoelasticity and cross-bridge kinetics

Myocardial viscoelasticity was measured at maximal activating [Ca^{2+}] (pCa 4.8) and submaximally activating [Ca^{2+}] (pCa 5.4). Average, representative measurements shown in Fig. 3 come from all strips that underwent the OM titration from 0 to 10 μM at a single pCa level. The large decrease in the magnitude of moduli values between the left and right panels stems from less cross-bridge binding at pCa 5.4 (Fig. 3, *B* and *D*) vs. pCa 4.8 (Fig. 3, *A* and *C*), thereby contributing a smaller viscoelastic mechanical signature at the lower tension values. Under both maximally activated and submaximally activated conditions, these moduli-frequency relationships were shifted toward lower frequencies at 1.0 μM [OM] compared to measurements without OM. As a whole, the characteristic peaks and dips in these moduli-frequency relationships indicate a broad metric of cross-bridge cycling kinetics (36), in which the shift toward lower frequencies arises from slower cross-bridge cycling at 1.0 μM [OM] for both pCa conditions (Fig. 3).

Moduli-frequency relationships were fitted to Eq. 1 to extract model parameters related to myocardial viscoelasticity (further discussed below) and the rate constants for cross-bridge recruitment (2πb; Fig. 4, *A* and *B*) and cross-bridge detachment (2πc; Fig. 4, *C* and *D*). These rate constants progressively slowed with increasing [OM] at both pCa levels. In addition, the rate constants for cross-bridge detachment were more sensitive to increasing [OM] than the recruitment rate constants (at both Ca^{2+} activation levels). Specifically, the rate constant for cross-bridge detachment began to slow significantly ($p < 0.05$; compared to the control strips) at [OM] $\geq$0.1 μM at pCa 5.4 and 4.8, but the rate constant of cross-bridge recruitment did not begin to slow significantly until [OM] $\geq$1 μM at pCa 5.4 and 4.8. Before the addition of OM, cross-bridge recruitment rate constants were similar at both pCa levels. However, cross-bridge detachment rate constants (before the addition of OM) were roughly 31% faster at submaximal (Fig. 4 *D*) versus maximal (Fig. 4 *C*) Ca^{2+} activation conditions. In concert with the steady-state tension data, these kinetics measurements show an interesting interplay between Ca^{2+} activation level and the effects of [OM] on

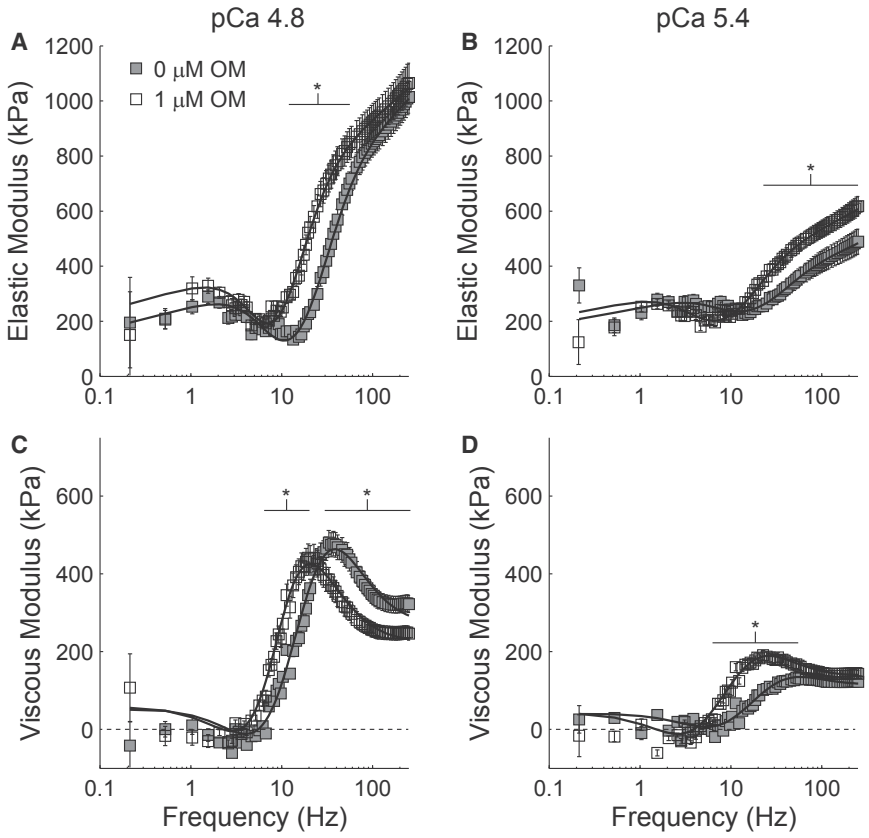

FIGURE 3 Elastic (*A* and *B*) and viscous (*C* and *D*) moduli values were plotted against frequency at maximal Ca^{2+} activation (pCa 4.8; *A* and *C*) and submaximal Ca^{2+} activation (pCa 5.4; *B* and *D*) for the OM-titrated strips at 0 and 1 μM [OM]. Number of strips: 21 at pCa 4.8, 20 at pCa 5.4. $^*p < 0.05$ frequencies where moduli values differed between 0 and 1 μM [OM] within each panel.

cross-bridge function that increases force production more at submaximal pCa levels.

The additional model parameters contributing to Eq. 1 represent relative changes in myocardial stiffness (Fig. 5, *A–D*) and the magnitude of cross-bridge binding (Fig. 5, *E–H*). There are minimal changes in viscoelastic myocardial stiffness arising from the passive elements of the sarcomere, with *A* and *k* values remaining largely unchanged as [OM] increased; these values were also similar between the OM-treated and control groups within either Ca^{2+} activation level (Fig. 5, *A–D*). At pCa 5.4, *k* values slightly increased at [OM] above 0.3 μM (Fig. 5 *D*), which represents a slightly greater viscous characteristic in the myocardium (i.e., a small shift from primarily elastic toward slightly less elastic in the relative viscoelastic properties of the tissue (31)). In combination, however, these *A*-process data suggest no major difference in the passive elements of the myofilaments that contribute to myocardial viscoelasticity at either Ca^{2+} activation level.

The magnitudes of *B* and *C* were relatively flat for the control (DMSO-only) group, suggesting no significant changes in number of bound cross-bridges or cross-bridge stiffness values across the range of solution exchanges at either pCa level (Fig. 5, *E–H*). The relative magnitudes for *B* and *C* were also less at submaximal (Fig. 5, *F* and *H*) versus maximal Ca^{2+} activation (Fig. 5, *E* and *G*), as would be anticipated with less cross-bridge binding and lower tension values at submaximal Ca^{2+} activation.

Under maximally activated conditions, OM-treated strips showed a biphasic response, with the magnitudes of *B* and *C* increasing as [OM] increased to 1 μM, then sharply decreasing above 1 μM [OM]. One would typically anticipate the relative magnitudes of *B* and *C* to scale with tension values, which is consistent between the sharp decreases in *B*, *C* (Fig. 5, *E* and *G*), and tension at the highest [OM] for pCa 4.8 (Fig. 2 *A*). At pCa 5.4, the magnitudes of *B* and *C* were relatively flat for both OM-treated strips (Fig. 5, *F* and *H*), which would typically suggest no significant change in magnitude of cross-bridge binding or net stiffness of attached cross-bridges as OM increased for pCa 5.4. Therefore, OM appears to be disconnecting the typical link between cross-bridge binding (i.e., magnitudes of *B* and *C*) and tension production, which alludes to more complicated cross-bridge activity or force-generating dynamic than typically observed.

DISCUSSION

Multiple theories have been proposed to explain the mechanism of action by which OM affects different chemomechanical steps of the cross-bridge cycle. Given that temperature is an important variable in regulating enzyme

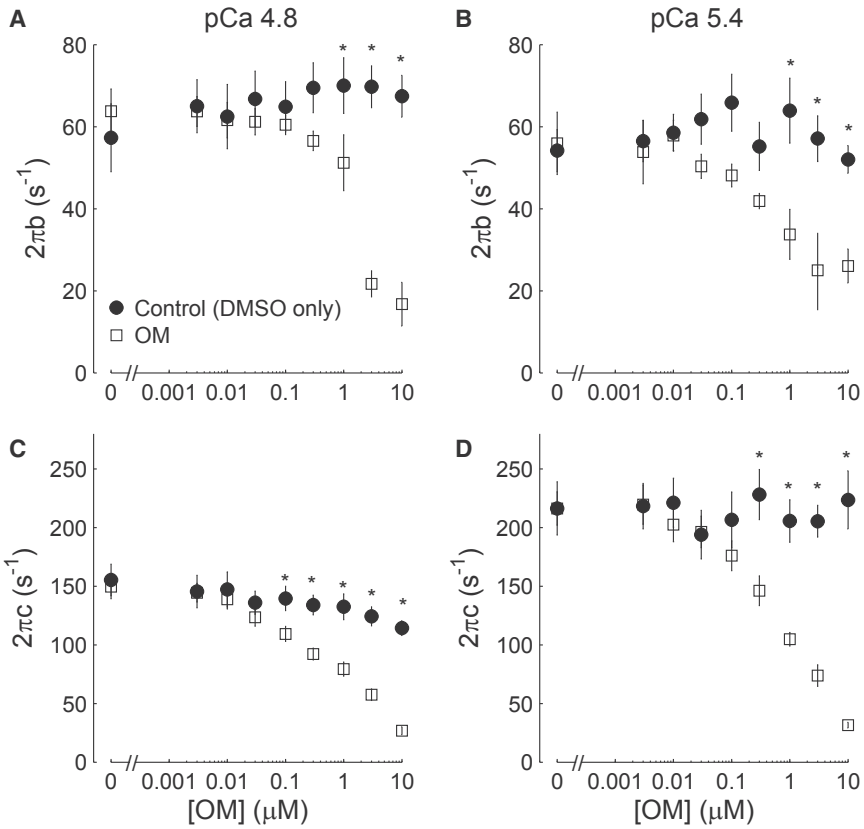

FIGURE 4 Effect of [OM] on cross-bridge recruitment (2πb; *A* and *B*) and cross-bridge detachment (2πc; *C* and *D*) at maximal (pCa 4.8; *A* and *C*) and submaximal (pCa 5.4; *B* and *D*) Ca^{2+} activation levels. Number of strips for each condition are listed in legend of Fig. 2. *$p < 0.05$ between the control and OM titration within each panel.

activity and physiological function, we investigated the effects of OM on cardiac muscle function and cross-bridge kinetics at physiological temperature (37°C). Previous muscle mechanics studies at subphysiological temperatures have shown mixed results for OM: 1) having no effect (16) or increasing (18,21,35) Ca^{2+} sensitivity of contraction and 2) having no effect (18), increasing (35), or decreasing (14,16) maximal tension. Some of these earlier studies, in combination with solution biochemistry experiments, suggested that OM augments contractility because of faster P_i release, even though myosin force production may be slowed at the weak-to-strong binding isomerization step of the cross-bridge cycle (11). In addition, OM has also been linked with greater contractility due to prolonged myosin detachment and increased myosin duty ratio (18,21,22,37). Our findings at physiological temperature show a strong consensus with these prior observations and help illustrate how molecular effects of OM augment myocardial contractility more at submaximal versus maximal Ca^{2+} activation levels (i.e., closer to physiological intracellular [Ca^{2+}]).

As previously observed (14,16,21), we found that the OM-dependent increases in isometric tension were inversely correlated with Ca^{2+} activation level. At 1 μM [OM], increases in force began around pCa 6–6.5, near the rising edge of the tension-pCa curve at the onset of contractile activation (Fig. 1). In addition, we also found that titrating [OM] for 0–10 μM led to increases in steady-state tension values solely at submaximal activation (pCa 5.4; Fig. 2 *B*). These different tension responses at different Ca^{2+} activation levels imply an interplay between the effects of [OM] on myosin cross-bridge binding and kinetics that influences cooperative activation of contraction.

Prior studies have also shown that OM consistently decreases the Hill coefficient and slows myosin rate transitions at one or more portions of the cross-bridge cycle (11,14,16–18,21,22,35). These general consistencies persist across multiple temperatures (15–37°C), ionic strengths (180–200 mM), and myriad assays using skeletal and cardiac myosin (single molecule, solution biochemistry, and skinned and intact muscle mechanics). Kamporakis et al. (16) used fluorescent probes on myosin regulatory light chain and troponin C to show that OM shifts myosin from the OFF to ON state (38–42), thereby favoring the disordered, relaxed state in which myosin can bind with actin more easily. Consistent with our findings, this bias toward the ON state provides a simple explanation for the decrease in Hill coefficient, in which OM increases tension values at submaximal Ca^{2+} activation levels to shift the lower portion of the tension-pCa relationship to the left, without affecting the top portion of the Ca^{2+}-activated tension response.

Woody et al. (22) put forth the hypothesis that OM may also increase the duration of time that OM-bound myosin cross-bridges remain attached with actin, even though these OM-bound bridges have a shorter or inhibited power stroke

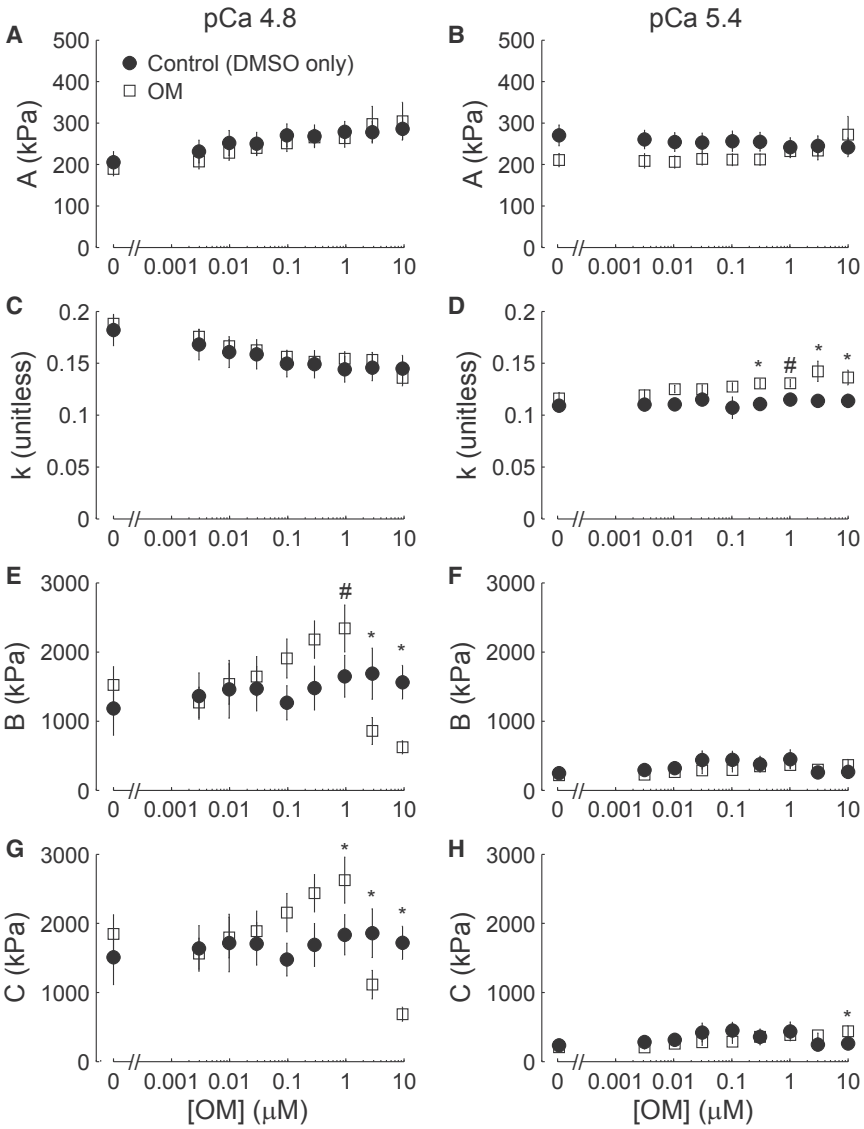

FIGURE 5 Effect of [OM] on parameter values *A*, *k*, *B*, and *C* at pCa 4.8 and 5.4. The parameter *A* represents myocardial viscoelastic stiffness from passive (nonenzymatic) elements of the myocardial tissue, which remained largely unchanged as [OM] increased at pCa 4.8 (*A*) or 5.4 (*B*). The parameter *k* represents the relative viscoelastic characteristic of the myocardium, which was not affected by [OM] at pCa 4.8 (*C*). At pCa 5.4 (*D*), *k* values became slightly greater at [OM] >0.1 μM versus control strips. The parameters *B* and *C* represent relative levels of cross-bridge binding, which showed a biphasic response as [OM] increased at pCa 4.8 (*E* and *G*). The effects of [OM] on *B* and *C* were minimal at pCa 5.4 (*F* and *H*), and their relative magnitudes were much lower than the pCa 4.8 values because of lower cross-bridge binding and tension values at submaximal Ca^{2+} activation. Number of strips for each condition are listed in legend of Fig. 2. $*p < 0.05$ and $\#p < 0.07$ between the control and OM titration within each panel.

distance. These authors suggest that a greater population of higher-duty-ratio OM-bound myosin bridges would act to cooperatively activate the thin filament at low [Ca^{2+}], which in turn recruits additional OM-free myosin cross-bridges to augment tension. Our kinetics data support this hypothesis (Fig. 4) in that OM slows cycling kinetics and prolongs myosin binding, which may contribute to greater tension and cooperative activation of contraction at submaximal Ca^{2+} activation levels. One may envision this mechanism working via strong cross-bridge contributions to thin-filament activation from a relatively small population of cross-bridges that are binding OM, thereby leading to cooperative recruitment of the neighboring cross-bridge population.

Associated simulations from Woody et al. (22) suggest that myocardial force production increases at intermediate [OM] because of cooperative recruitment of additional cross-bridges that do not bind OM. These authors also describe an alternative actin-myosin dissociation pathway with OM that occurs before ADP release and helps explain why force may be inhibited at high [OM] regardless of Ca^{2+} activation level. This proposed mechanism would begin to separate the tight coupling between myocardial stiffness due to additional cross-bridge binding and active tension generation by this greater population of cross-bridges. Our measurements of viscoelastic stiffness, estimates of cross-bridge binding (i.e., the magnitudes of *B* and *C* values), and steady-state tension values also show some atypical disconnect between these processes but only in the presence of OM (Figs. 2 and 5). Given that our system analysis techniques require a mechanical signature (i.e., weak or strong cross-bridge contributions to viscoelastic myocardial stiffness), the slower rates of cross-bridge recruitment that we measure are consistent with bridges showing a slower

weak-to-strong isomerization step of the cross-bridge cycle (11,20,22). The concept of bound bridges that do not produce force or generate a smaller power stroke (or atypical detachment pathway (22)) may contribute to the small yet statistically significant increases in k values at pCa 5.4 for the highest [OM] (Fig. 5 *C*). Typically, slowed cross-bridge cycling kinetics (such as a titration toward rigor from saturating [MgATP] that slows kinetics) show a decreased magnitude for k due to increased cross-bridge recruitment and tension generation (31,36,43). However, we find the opposite, an increase in k even though there are increases in tension (~10–20%), which may be due to the greater population of OM-bound bridges contributing a mechanical signature typically consistent with fewer, slower-cycling (or static) force-generating cross-bridges. This separation between viscoelastic mechanical stiffness and tension suggests that OM-bound cross-bridges show increasingly slower-cycling kinetics (i.e., weak-to-strong recruitment transitions and slowed detachment), even though there may be increased OM-bound bridges that do not produce a "force-generating" power stroke.

At maximal activation, the relative fraction of OM-bound bridges to total bound cross-bridges may also be rather small, and thus, we observe a biphasic response of cross-bridge contributions to myocardial stiffness (Fig. 5, *E* and *G*) even though the associated tension response was relatively flat and only decreased at the highest [OM] (Fig. 2 *A*). By comparison, the relative cross-bridge binding and associated cross-bridge contribution to myocardial stiffness was much lower at submaximal activation (Fig. 5, *F* and *H*). Consequently, the biphasic tension response at submaximal tension that follows from cooperative cross-bridge contributions to activation and force production (Fig. 2 *B*) only produced modest increases in force compared to the doubling of force between pCa 5.4 and 4.8. Building on the predictions from Woody et al. (22) and the slowed kinetics due to OM-bound cross-bridges, one may begin to envisage a more static and less-efficient system of motors, thus suggesting diminished contractility among a subset of motors that are binding OM to enhance overall ensemble motor function and slightly augment contraction at submaximal Ca^{2+} levels.

Gollapudi et al. (35) investigated sarcomere length-dependent effects of OM in skinned guinea pig papillary muscle and also found a decrease in the Hill coefficient and slower cross-bridge kinetics (at both short (1.9 μm) and long (2.2 μm) sarcomere lengths). As myocardium is stretched to longer sarcomere lengths, it typically shows increased maximal force and Ca^{2+} sensitivity of contraction; this response is called length-dependent activation of contraction (44–48). Surprisingly, OM eliminated length-dependent activation in that calcium-sensitivity of the tension-pCa relationship was similar at short and long sarcomere lengths in the presence of OM (35). These authors also reported that OM increased the number of force-bearing cross-bridges significantly at short sarcomere length but not at long sarcomere length. Compared to controls (no OM), OM also induced greater increases in myofilament Ca^{2+} sensitivity at short versus long sarcomere length. We believe these observations of Gollapudi et al. make more sense in the context of OM, and length-dependent force increases both modulating the mechanosensitive myosin OFF-ON equilibrium. Given that OM and force both destabilize the myosin OFF state (16,49), the relative effects of OM on the tension-pCa relationship will be greatest at the shortest sarcomere lengths because the heads will have already been destabilized via greater tension values at the longer sarcomere length.

Given the different effects of OM on tension development between submaximal and maximal Ca^{2+} activation levels (Fig. 2), we were somewhat surprised to see that the relative changes in cross-bridge kinetics due to increasing [OM] were largely similarly between pCa 4.8 and 5.4 (Fig. 4). Specifically, cross-bridge recruitment rate constants were ~60 s^{-1} in the absence of OM, and then decreased to ~20 s^{-1} (roughly a 60% reduction) at both Ca^{2+} activation levels. In the absence of OM, the rate constant for cross-bridge detachment was slightly slower at pCa 4.8 (~150 s^{-1}) versus pCa 5.4 (~220 s^{-1}), which may indicate an interplay between thin-filament activation levels and cross-bridge detachment rate kinetics at physiological temperature (further discussed below). Nonetheless, cross-bridge detachment kinetics decreased sharply as [OM] increased, to ~25 s^{-1} at 10 μM [OM] (an 80–85% reduction) for both pCa levels (Fig. 4, *C* and *D*). These data suggest that OM-dependent slowing of cross-bridge cycling prolongs myosin attachment duration to augment cooperative activation of contraction in a similar manner at both submaximal and maximal activation levels. However, the tension data show that this cooperative activation of contraction only augments tension at submaximal Ca^{2+} activation levels because thin-filament activation and force production are already saturated at pCa 4.8.

Independent of [OM], the rate of cross-bridge detachment was ~46% slower at maximal (pCa 4.8) versus submaximal (pC 5.4) activation levels (Fig. 4, *C–D*). Similar findings for these Ca^{2+}-dependent detachment kinetics have been shown for human myocardial strips at physiological temperature (50), as well as rat cardiac and skeletal muscle measurements from our laboratory at subphysiological temperatures (23,36,51). These data suggest that Ca^{2+} activation levels may influence cross-bridge detachment kinetics. Other measurements of myosin kinetics use a technique that shortens and restretches the muscle to its original length to observe an apparent rate of tension recovery (k_{tr}), showing that k_{tr} increases nonlinearly with increasing [Ca^{2+}] (52,53). This single apparent k_{tr} value is thought to reflect the summation of both rate constants for cross-bridge attachment and detachment (in terms of Huxley's f and g definitions (54)). The nonlinear increase in k_{tr} has been interpreted as a

Ca^{2+}-dependent increase in the rate constant for cross-bridge attachment that is limited by Ca^{2+} binding to troponin and the additional kinetic steps underlying thin-filament activation and that the associated rate constant for cross-bridge detachment was not Ca^{2+} dependent (52,55). In contrast, these sinusoidal or stochastic system analysis measurements do not consistently show effects of Ca^{2+} activation on the rate of cross-bridge recruitment (Fig. 4), partly because these measurements require, at a minimum, cross-bridges to be weakly bound to contribute a mechanical signature constituting the stress-strain response of a modulus value. Altogether, these techniques are useful to assess dynamic cross-bridge behavior but may sample different contributions to the thin-filament versus thick-filament regulatory processes underlying cooperative activation of contraction.

Previously, we observed slower rates of cross-bridge detachment at longer sarcomere length, with force also greater at the longer sarcomere length (23,36,51). We have largely interpreted these length-dependent differences to stem from strain-dependent differences in cross-bridge cycling, in which length-dependent tension increases led to slower detachment at longer sarcomere lengths because of slowed ADP dissociation rates (as the bridges bear greater strain and force). We found no effect of sarcomere length on the rate of cross-bridge recruitment, even though tension and cross-bridge strain can influence both recruitment and detachment kinetics (32,33). Thus, the sarcomere-length-dependent (i.e., tension or strain-dependent) kinetic behaviors that we observed previously are analogous to the Ca^{2+}-dependent (i.e., tension or strain-dependent) kinetic behaviors measured herein in the absence of OM (Fig. 4). Most studies of length-dependent cross-bridge kinetics used relatively large amplitude k_{tr} release-restretch protocols, compared to the very low amplitude strains used for stochastic length perturbation analysis. Slower k_{tr} values were observed at longer sarcomere length (56–61), and because k_{tr} is thought to be a summation of the cross-bridge attachment and cross-bridge detachment rates (53), our prior studies (23,36,51) support the idea that k_{tr} decreases with sarcomere length because of slowed cross-bridge detachment rate without affecting cross-bridge attachment rate (56,61).

However, the predominant view of muscle activation entails 1) tropomyosin blocking the target sites for myosin binding along the thin filaments in the absence of calcium, 2) increases in Ca^{2+}-troponin binding further shifting tropomyosin across the thin filament to expose target sites on actin for strong myosin binding, and 3) that myosin binding further shifts or opens tropomyosin position to stabilize exposed target sites on actin, thereby augmenting activation and myosin binding (62–65). This steric blocking model supports the idea that Ca^{2+}-dependent increases in k_{tr} are limited by myosin attachment rates as thin-filament activation increases (52,55), and other biochemical, single-molecule, and ensemble myosin studies show that myosin cross-bridge ADP dissociation rates are not differentially affected via thin-filament regulatory proteins (66,67). Similar biochemical studies suggest that ADP release rates (akin to the cross-bridge detachment rate measured herein) are $\sim$500 s^{-1} near physiological temperature (68,69), which is 2- to 3-fold faster than our measurements in skinned myocardial strips (Fig. 4). There are limited data (to our current knowledge) supporting our interpretation of Ca^{2+}-dependent cross-bridge detachment rates, as discussed just above. This could arise from a limited representation or explanation in our current model (Eq. 1) describing the cross-bridge activity that underlies frequency-dependent viscoelastic system analysis data (Fig. 3–5), though these observations show internal consistency with cross-bridge kinetics reported in prior sinusoidal analysis studies at physiological temperature (50). Thus, there may be a secondary contribution to the observed kinetics that is couched in the relative temperature sensitivities of Ca^{2+} binding and thin-filament activation and deactivation dynamics versus cross-bridge cycling kinetics.

At subphysiological temperatures, the rates of Ca^{2+} activation and deactivation of the thin filament are much faster than the rates of cross-bridge association and dissociation from actin (70–72). Therefore, Ca^{2+} has typically been thought of as the switch that activates contractility, and the slower cross-bridge detachment may be the rate-limiting step for myofilament deactivation and relaxation (73). However, Ca^{2+}-troponin C binding and dissociation kinetics are not as temperature sensitive as cross-bridge cycling kinetics (43,70–72,74), and with the addition of complexity (such as troponin + topomyosin + myosin S1 or cross-bridges), the relative activation and deactivation kinetics slow down by a couple orders of magnitude (75–78). At physiological temperatures, the rates of cross-bridge attachment and detachment may be governed by strain-dependent or tension-dependent cross-bridge mechanisms, more so than Ca^{2+} activation and deactivation dynamics along the thin filament. The Ca^{2+}-dependent detachment kinetics that we measured in the absence of OM may stem from both tension-dependent and temperature-dependent sensitivities for cross-bridge behavior, in which thin-filament activation and deactivation kinetics are less dependent upon tension and temperature. Given the exciting developments of 1) dynamic regulation of activation between the thick and thin filaments and 2) a mechanosensitive equilibrium between the super-relaxed and disordered-relaxed states, the intrinsic myofilament processes that govern cross-bridge activation, force production, and efficient utilization of ATP throughout a contraction-relaxation cycle combine to represent an exciting "regulation renaissance" in muscle biophysics and physiology that requires more detailed and focused attention to perceive in full (41,79,80).

Although the greatest effects of OM on myocardial contraction occur at the highest [OM] that we tested

(1–10 μM), OM begins to alter rate constants for myosin cross-bridge detachment at [OM] = 100–300 nM at physiological temperature (Fig. 4). It should be noted that the relative sensitivity to [OM] may also depend upon pCa level (14,18,35), by which the effect of the drug begins to alter contractility and cross-bridge kinetics at [OM] $\leq$100 nM at submaximal activation levels (i.e., closer to physiological [Ca^{2+}] (81,82)) but requires higher concentrations (300–500 nM) to influence contractility and cross-bridge kinetics at maximal activation (Figs. 2 and 4). Given that estimated therapeutic plasma [OM] range from 200 to 800 nM in patients (9,10), these findings clarify potential therapeutic implications for drug delivery and help to extend design parameters guiding small-molecule therapies to alter myosin activity and myocardial force production.

AUTHOR CONTRIBUTIONS

All of the authors designed the research study, analyzed data, and wrote the manuscript. T.T.K. and P.O.A. performed the experiments.

ACKNOWLEDGMENTS

We thank Axel Fenwick and David Dewitt for their comments on the earlier versions of this manuscript.

This research was supported by an Auvil Research Scholars Fellowship to T.T.K. and grants from the American Heart Association (17SDG33370153) and National Science Foundation (1656450) to B.C.W.T.

REFERENCES

1. Lymn, R. W., and E. W. Taylor. 1971. Mechanism of adenosine triphosphate hydrolysis by actomyosin. *Biochemistry.* 10:4617–4624.
2. Goldman, Y. E. 1987. Kinetics of the actomyosin ATPase in muscle fibers. *Annu. Rev. Physiol.* 49:637–654.
3. Benjamin, E. J., S. S. Virani, …, P. Muntner; American Heart Association Council on Epidemiology and Prevention Statistics Committee and Stroke Statistics Subcommittee. 2018. Heart disease and stroke statistics-2018 update: a report from the American Heart Association. *Circulation.* 137:e67–e492.
4. van Riet, E. E., A. W. Hoes, …, F. H. Rutten. 2016. Epidemiology of heart failure: the prevalence of heart failure and ventricular dysfunction in older adults over time. A systematic review. *Eur. J. Heart Fail.* 18:242–252.
5. Redfield, M. M., S. J. Jacobsen, …, R. J. Rodeheffer. 2003. Burden of systolic and diastolic ventricular dysfunction in the community: appreciating the scope of the heart failure epidemic. *JAMA.* 289:194–202.
6. Owan, T. E., D. O. Hodge, …, M. M. Redfield. 2006. Trends in prevalence and outcome of heart failure with preserved ejection fraction. *N. Engl. J. Med.* 355:251–259.
7. Malik, F. I., J. J. Hartman, …, D. J. Morgans. 2011. Cardiac myosin activation: a potential therapeutic approach for systolic heart failure. *Science.* 331:1439–1443.
8. Kaplinsky, E., and G. Mallarkey. 2018. Cardiac myosin activators for heart failure therapy: focus on omecamtiv mecarbil. *Drugs Context.* 7:212518.
9. Teerlink, J. R., C. P. Clarke, …, A. A. Wolff. 2011. Dose-dependent augmentation of cardiac systolic function with the selective cardiac myosin activator, omecamtiv mecarbil: a first-in-man study. *Lancet.* 378:667–675.
10. Teerlink, J. R., G. M. Felker, …, N. Honarpour; COSMIC-HF Investigators. 2016. Chronic oral study of myosin activation to increase contractility in heart failure (COSMIC-HF): a phase 2, pharmacokinetic, randomised, placebo-controlled trial. *Lancet.* 388:2895–2903.
11. Rohde, J. A., D. D. Thomas, and J. M. Muretta. 2017. Heart failure drug changes the mechanoenzymology of the cardiac myosin powerstroke. *Proc. Natl. Acad. Sci. USA.* 114:E1796–E1804.
12. Winkelmann, D. A., E. Forgacs, …, A. M. Stock. 2015. Structural basis for drug-induced allosteric changes to human β-cardiac myosin motor activity. *Nat. Commun.* 6:7974.
13. Liu, Y., H. D. White, …, E. Forgacs. 2015. Omecamtiv Mecarbil modulates the kinetic and motile properties of porcine β-cardiac myosin. *Biochemistry.* 54:1963–1975.
14. Nagy, L., Á. Kovács, …, Z. Papp. 2015. The novel cardiac myosin activator omecamtiv mecarbil increases the calcium sensitivity of force production in isolated cardiomyocytes and skeletal muscle fibres of the rat. *Br. J. Pharmacol.* 172:4506–4518.
15. Planelles-Herrero, V. J., J. J. Hartman, …, A. Houdusse. 2017. Mechanistic and structural basis for activation of cardiac myosin force production by omecamtiv mecarbil. *Nat. Commun.* 8:190.
16. Kampourakis, T., X. Zhang, …, M. Irving. 2018. Omecamtiv mercabil and blebbistatin modulate cardiac contractility by perturbing the regulatory state of the myosin filament. *J. Physiol.* 596:31–46.
17. Mamidi, R., J. Li, …, J. E. Stelzer. 2017. Dose-dependent effects of the myosin activator omecamtiv mecarbil on cross-bridge behavior and force generation in failing human myocardium. *Circ Heart Fail.* 10:e004257.
18. Swenson, A. M., W. Tang, …, C. M. Yengo. 2017. Omecamtiv mecarbil enhances the duty ratio of human β-cardiac myosin resulting in increased calcium sensitivity and slowed force development in cardiac muscle. *J. Biol. Chem.* 292:3768–3778.
19. Wang, L., X. Ji, …, M. Kawai. 2014. Phosphorylation of cMyBP-C affects contractile mechanisms in a site-specific manner. *Biophys. J.* 106:1112–1122.
20. Liu, C., M. Kawana, …, J. A. Spudich. 2018. Controlling load-dependent kinetics of β-cardiac myosin at the single-molecule level. *Nat. Struct. Mol. Biol.* 25:505–514.
21. Mamidi, R., K. S. Gresham, …, J. E. Stelzer. 2015. Molecular effects of the myosin activator omecamtiv mecarbil on contractile properties of skinned myocardium lacking cardiac myosin binding protein-C. *J. Mol. Cell. Cardiol.* 85:262–272.
22. Woody, M. S., M. J. Greenberg, …, E. M. Ostap. 2018. Positive cardiac inotrope omecamtiv mecarbil activates muscle despite suppressing the myosin working stroke. *Nat. Commun.* 9:3838.
23. Pulcastro, H. C., P. O. Awinda, …, B. C. Tanner. 2016. Effects of myosin light chain phosphorylation on length-dependent myosin kinetics in skinned rat myocardium. *Arch. Biochem. Biophys.* 601:56–68.
24. Tanner, B. C., Y. Wang, …, B. M. Palmer. 2011. Measuring myosin cross-bridge attachment time in activated muscle fibers using stochastic vs. sinusoidal length perturbation analysis. *J. Appl. Physiol. (1985).* 110:1101–1108.
25. Godt, R. E., and B. D. Lindley. 1982. Influence of temperature upon contractile activation and isometric force production in mechanically skinned muscle fibers of the frog. *J. Gen. Physiol.* 80:279–297.
26. Kurebayashi, N., and Y. Ogawa. 1985. Effect of quercetin on tension development by skinned fibres from frog skeletal muscle. *J. Muscle Res. Cell Motil.* 6:189–195.
27. Reid, M. B., and M. R. Moody. 1994. Dimethyl sulfoxide depresses skeletal muscle contractility. *J. Appl. Physiol.* 76:2186–2190.
28. Velasco, R., X. Trujillo, …, B. Trujillo-Hernández. 2003. Effect of dimethyl sulfoxide on excitation-contraction coupling in chicken slow skeletal muscle. *J. Pharmacol. Sci.* 93:149–154.
29. Kawai, M., and P. W. Brandt. 1980. Sinusoidal analysis: a high resolution method for correlating biochemical reactions with physiological processes in activated skeletal muscles of rabbit, frog and crayfish. *J. Muscle Res. Cell Motil.* 1:279–303.

30. Palmer, B. M., T. Suzuki, …, D. W. Maughan. 2007. Two-state model of acto-myosin attachment-detachment predicts C-process of sinusoidal analysis. *Biophys. J.* 93:760–769.

31. Palmer, B. M., B. C. Tanner, …, M. S. Miller. 2013. An inverse power-law distribution of molecular bond lifetimes predicts fractional derivative viscoelasticity in biological tissue. *Biophys. J.* 104:2540–2552.

32. Palmer, B. M. 2010. A strain-dependency of Myosin off-rate must be sensitive to frequency to predict the B-process of sinusoidal analysis. *Adv. Exp. Med. Biol.* 682:57–75.

33. Palmer, B. M., Y. Wang, and M. S. Miller. 2011. Distribution of myosin attachment times predicted from viscoelastic mechanics of striated muscle. *J. Biomed. Biotechnol.* 2011:592343.

34. Campbell, K. B., M. Chandra, …, W. C. Hunter. 2004. Interpreting cardiac muscle force-length dynamics using a novel functional model. *Am. J. Physiol. Heart Circ. Physiol.* 286:H1535–H1545.

35. Gollapudi, S. K., S. M. Reda, and M. Chandra. 2017. Omecamtiv mecarbil abolishes length-mediated increase in Guinea pig cardiac myofiber Ca2+ sensitivity. *Biophys. J.* 113:880–888.

36. Tanner, B. C., J. J. Breithaupt, and P. O. Awinda. 2015. Myosin MgADP release rate decreases at longer sarcomere length to prolong myosin attachment time in skinned rat myocardium. *Am. J. Physiol. Heart Circ. Physiol.* 309:H2087–H2097.

37. Aksel, T., E. Choe Yu, …, J. A. Spudich. 2015. Ensemble force changes that result from human cardiac myosin mutations and a small-molecule effector. *Cell Reports.* 11:910–920.

38. Linari, M., E. Brunello, …, M. Irving. 2015. Force generation by skeletal muscle is controlled by mechanosensing in myosin filaments. *Nature.* 528:276–279.

39. Kampourakis, T., Y.-B. Sun, and M. Irving. 2016. Myosin light chain phosphorylation enhances contraction of heart muscle via structural changes in both thick and thin filaments. *Proc. Natl. Acad. Sci. USA.* 113:E3039–E3047.

40. Fusi, L., E. Brunello, …, M. Irving. 2016. Thick filament mechanosensing is a calcium-independent regulatory mechanism in skeletal muscle. *Nat. Commun.* 7:13281.

41. Piazzesi, G., M. Caremani, …, V. Lombardi. 2018. Thick filament mechano-sensing in skeletal and cardiac muscles: a common mechanism able to adapt the energetic cost of the contraction to the task. *Front. Physiol.* 9:736.

42. Zhang, X., T. Kampourakis, …, Y.-B. Sun. 2017. Distinct contributions of the thin and thick filaments to length-dependent activation in heart muscle. *eLife.* 6:e24081.

43. Wang, Y., B. C. Tanner, …, B. M. Palmer. 2013. Cardiac myosin isoforms exhibit differential rates of MgADP release and MgATP binding detected by myocardial viscoelasticity. *J. Mol. Cell. Cardiol.* 54:1–8.

44. Allen, D. G., and J. C. Kentish. 1985. The cellular basis of the length-tension relation in cardiac muscle. *J. Mol. Cell. Cardiol.* 17:821–840.

45. Bers, D. M. 2001. Excitation-Contraction Coupling and Cardiac Contractile Force. Kluwer Academic Press, Dordrecht, The Netherlands.

46. Campbell, K. S. 2011. Impact of myocyte strain on cardiac myofilament activation. *Pflugers Arch.* 462:3–14.

47. Sagawa, K., L. Maughan, …, K. Sunagawa. 1988. Cardiac Contraction and the Pressure-Volume Relationship. Oxford University Press, New York.

48. de Tombe, P. P., R. D. Mateja, …, T. C. Irving. 2010. Myofilament length dependent activation. *J. Mol. Cell. Cardiol.* 48:851–858.

49. Campbell, K. S., P. M. L. Janssen, and S. G. Campbell. 2018. Force-dependent recruitment from the myosin off state contributes to length-dependent activation. *Biophys. J.* 115:543–553.

50. Donaldson, C., B. M. Palmer, …, M. M. LeWinter. 2012. Myosin cross-bridge dynamics in patients with hypertension and concentric left ventricular remodeling. *Circ Heart Fail.* 5:803–811.

51. Fenwick, A. J., S. R. Leighton, and B. C. W. Tanner. 2016. Myosin MgADP release rate decreases as sarcomere length increases in skinned rat soleus muscle fibers. *Biophys. J.* 111:2011–2023.

52. Brenner, B., and E. Eisenberg. 1986. Rate of force generation in muscle: correlation with actomyosin ATPase activity in solution. *Proc. Natl. Acad. Sci. USA.* 83:3542–3546.

53. Brenner, B. 1988. Effect of Ca2+ on cross-bridge turnover kinetics in skinned single rabbit psoas fibers: implications for regulation of muscle contraction. *Proc. Natl. Acad. Sci. USA.* 85:3265–3269.

54. Huxley, A. F. 1957. Muscle structure and theories of contraction. *Prog. Biophys. Biophys. Chem.* 7:255–318.

55. Gordon, A. M., E. Homsher, and M. Regnier. 2000. Regulation of contraction in striated muscle. *Physiol. Rev.* 80:853–924.

56. Adhikari, B. B., and K. Wang. 2004. Interplay of troponin- and Myosin-based pathways of calcium activation in skeletal and cardiac muscle: the use of W7 as an inhibitor of thin filament activation. *Biophys. J.* 86:359–370.

57. Hanft, L. M., M. L. Greaser, and K. S. McDonald. 2014. Titin-mediated control of cardiac myofibrillar function. *Arch. Biochem. Biophys.* 552-553:83–91.

58. Korte, F. S., and K. S. McDonald. 2007. Sarcomere length dependence of rat skinned cardiac myocyte mechanical properties: dependence on myosin heavy chain. *J. Physiol.* 581:725–739.

59. Milani-Nejad, N., Y. Xu, …, P. M. Janssen. 2013. Effect of muscle length on cross-bridge kinetics in intact cardiac trabeculae at body temperature. *J. Gen. Physiol.* 141:133–139.

60. Patel, J. R., J. M. Pleitner, …, M. L. Greaser. 2012. Magnitude of length-dependent changes in contractile properties varies with titin isoform in rat ventricles. *Am. J. Physiol. Heart Circ. Physiol.* 302:H697–H708.

61. Stelzer, J. E., and R. L. Moss. 2006. Contributions of stretch activation to length-dependent contraction in murine myocardium. *J. Gen. Physiol.* 128:461–471.

62. McKillop, D. F., and M. A. Geeves. 1993. Regulation of the interaction between actin and myosin subfragment 1: evidence for three states of the thin filament. *Biophys. J.* 65:693–701.

63. Geeves, M. A., and S. S. Lehrer. 2002. Modeling thin filament cooperativity. *Biophys. J.* 82:1677–1681.

64. Maytum, R., S. S. Lehrer, and M. A. Geeves. 1999. Cooperativity and switching within the three-state model of muscle regulation. *Biochemistry.* 38:1102–1110.

65. Vibert, P., R. Craig, and W. Lehman. 1997. Steric-model for activation of muscle thin filaments. *J. Mol. Biol.* 266:8–14.

66. Sommese, R. F., S. Nag, …, K. M. Ruppel. 2013. Effects of troponin T cardiomyopathy mutations on the calcium sensitivity of the regulated thin filament and the actomyosin cross-bridge kinetics of human β-cardiac myosin. *PLoS One.* 8:e83403.

67. Longyear, T., S. Walcott, and E. P. Debold. 2017. The molecular basis of thin filament activation: from single molecule to muscle. *Sci. Rep.* 7:1822.

68. Deacon, J. C., M. J. Bloemink, …, L. A. Leinwand. 2012. Identification of functional differences between recombinant human α and β cardiac myosin motors. *Cell. Mol. Life Sci.* 69:2261–2277.

69. Walklate, J., Z. Ujfalusi, and M. A. Geeves. 2016. Myosin isoforms and the mechanochemical cross-bridge cycle. *J. Exp. Biol.* 219:168–174.

70. Dong, W., S. S. Rosenfeld, …, H. C. Cheung. 1996. Kinetic studies of calcium binding to the regulatory site of troponin C from cardiac muscle. *J. Biol. Chem.* 271:688–694.

71. Little, S. C., B. J. Biesiadecki, …, J. P. Davis. 2012. The rates of Ca2+ dissociation and cross-bridge detachment from ventricular myofibrils as reported by a fluorescent cardiac troponin C. *J. Biol. Chem.* 287:27930–27940.

72. Tikunova, S. B., and J. P. Davis. 2004. Designing calcium-sensitizing mutations in the regulatory domain of cardiac troponin C. *J. Biol. Chem.* 279:35341–35352.

73. Janssen, P. M., L. B. Stull, and E. Marbán. 2002. Myofilament properties comprise the rate-limiting step for cardiac relaxation at body temperature in the rat. *Am. J. Physiol. Heart Circ. Physiol.* 282:H499–H507.

74. de Tombe, P. P., and G. J. Stienen. 2007. Impact of temperature on cross-bridge cycling kinetics in rat myocardium. *J. Physiol.* 584:591–600.

75. Solzin, J., B. Iorga, …, R. Stehle. 2007. Kinetic mechanism of the Ca2+-dependent switch-on and switch-off of cardiac troponin in myofibrils. *Biophys. J.* 93:3917–3931.

76. Davis, J. P., J. A. Rall, …, S. B. Tikunova. 2004. Mutations of hydrophobic residues in the N-terminal domain of troponin C affect calcium binding and exchange with the troponin C-troponin I96-148 complex and muscle force production. *J. Biol. Chem.* 279:17348–17360.

77. Tesi, C., N. Piroddi, …, C. Poggesi. 2002. Relaxation kinetics following sudden Ca(2+) reduction in single myofibrils from skeletal muscle. *Biophys. J.* 83:2142–2151.

78. Siemankowski, R. F., M. O. Wiseman, and H. D. White. 1985. ADP dissociation from actomyosin subfragment 1 is sufficiently slow to limit the unloaded shortening velocity in vertebrate muscle. *Proc. Natl. Acad. Sci. USA.* 82:658–662.

79. Irving, M. 2017. Regulation of contraction by the thick filaments in skeletal muscle. *Biophys. J.* 113:2579–2594.

80. Campbell, K. S. 2017. Super-relaxation helps muscles work more efficiently. *J. Physiol.* 595:1007–1008.

81. Bassani, J. W., R. A. Bassani, and D. M. Bers. 1995. Calibration of indo-1 and resting intracellular [Ca]i in intact rabbit cardiac myocytes. *Biophys. J.* 68:1453–1460.

82. Gao, W. D., N. G. Perez, and E. Marban. 1998. Calcium cycling and contractile activation in intact mouse cardiac muscle. *J. Physiol.* 507:175–184.